International Journal of Advance Interdisciplinary Research
Vol. 2, Issue 2, Part A, April-June) 2026, pp. 1-13, e-ISSN: 3107-913X
DOI:https://doi.org/10.66095/ijair.2026.v2.i2.a.1

Thermoelastic properties of $BiFeO_3$ under different pressure conditions

Nidhi Gond[1], Shipra Tripathi[1], Anjani K Pandey[2], Chandra K Dixit[1]
[1]Dept of Physics, Dr. Shakuntala Misra National Rehabilitation University, Lucknow (India)
[2]Institute of Engineering and Technology, Dr. Shakuntala Misra National Rehabilitation University, Lucknow (India)
Email: gondnidhi56@gmail.com

Abstract

Bismuth ferrite ($BiFeO_3$) is a ubiquitously researched room-temperature multiferroic perovskite, which is simultaneously a ferroelectric, antiferromagnetic and ferro elastic ordering. Its pressure stability is of specific concern to possible use in memory devices, spintronics, and energy conversion technologies. In this paper, thermoelastic and pressure-dependent thermodynamic properties of $BiFeO_3$ are systematically studied by means of a combination of first-principles data and thermodynamic modeling using multiple equations of state (EOS) to Shanker, Poirier Tarantola, Bardeen and Srivastava-Pandey formulations, to provide a strong cross-validation of results. The development of pressure of bulk modulus, shear modulus has been investigated to distinguish anisotropic responses of elasticity and mechanical stability measures. Computed quantities like Gruneisen parameter and Lattice constant were solved at different compression, noting the interplay between lattice dynamics and elastic stiffness. Findings indicate that elastic moduli increase continuously with pressure, which means that the structural rhombohedral phase is more incompressible and stable until a critical pressure is reached at which new structural instabilities may occur. Gruneisen parameter decreases with pressure, which indicates a decrease in anharmonicity of lattice vibration. The results of these studies can be of great use in the elastic thermodynamic interaction of $BiFeO_3$ at extreme temperatures.

Key words: Isothermal EOS, Bulk Modulus, Lattice Constant, Gruneisen Parameter.

1. Introduction:

Substances that exhibit two or more ferroic orders, e.g. ferroelectricity, ferromagnetism, and ferroelasticity, are referred to as multiferroics. Certain materials are ferroelectric materials, that is, with no external electric field, they exhibit spontaneous electric polarization, or a natural separation of positive and negative charges. The key characteristic which makes a ferroelectric substance special is the capability to reverse or switch this spontaneous polarization under the influence of some outside electrical field. Some materials show the effect of antiferroelectricity, where no net macroscopic polarization occurs at zero external electric field due to oppositely oriented dipoles (electric moments) (antiparallel). In other words, in antiferroelectric AFE materials, the dipoles are orthogonal, the same

way as in ferroelectric FE materials, the dipoles are parallel. The AFE behaviour was first reported by Shirane et al. [1] to occur below 230 K2 in $PbZrO_3$. Subsequently, $PbHfO_3$ and other materials- $NaNbO_3$, $AgNbO_3$, $Pb(Mg_{0.5}W_{0.5})O_3$, $Pb(Yb_{0.5}Nb_{0.5})O3^{3-7}$ were found to exhibit anti-ferroelectricity [2]. Antiferroelectric materials have recently gained much research attention as a result of their enormous strain, giant electrocaloric effect, ultrahigh energy density and other encouraged features. Due to the good ferroelectric and magnetic ordering at room temperature, the bismuth ferrite ($BiFeO_3$) has emerged as one of the best multiferroic oxides. $BiFeO_3$ forms in a distorted perovskite form (ABO_3 -type) [3] with the oxygen octahedra forming the orientation of the occupancy of the A-site by Bi^{3+} ions and that of the B-site by Fe^{3+} ions. It is mainly the stereochemical activity of the $6s^2$ lone pair electrons of Bi^{3+} ions that migrate out of their centrosymmetric site and induce a spontaneous polarization that is the major source of ferroelectricity in $BiFeO_3$. On the other hand, the half-filled Fe^{3+} ($3d^5$) orbitals of the B-site favour antiferromagnetic order. $BiFeO_3$ is a simplified model system to study the phenomenon of magnetoelectric coupling since both types of ferroic orders exist in the identical phase. $BiFeO_3$ takes on a rhombohedral distorted perovskite structure with space group R3c at room temperature. [4] The possible applications of $BiFeO_3$ in many-purpose devices have also raised extensive research attention. Its strong ferroelectric-magnetic interaction presents possibilities of sensors, spintronics and memory devices. In addition, $BiFeO_3$ possesses an outstanding photovoltaic, electrochemical and catalytic properties which extends its application in energy storage, photocatalysis, and harvesting system. The disadvantages of $BiFeO_3$ despite these advantages are: it has high leakage current, spiral spin modulation, and high pressure structural instability. In order to overcome these limitations and enhance its properties in device applications, several methods have been employed including chemical doping, strain engineering in thin film, and nanostructuring. Investigations of the high-pressure of $BiFeO_3$ further improve our understanding of the underlying physics of this material and, specifically, display interesting structural changes and shifts in the ferroic properties. Therefore, $BiFeO_3$ shows good prospects in the future of multifunctional and energy-associated applications as it possesses distinct magnetic ordering, high ferroelectric polarization, and multifunctional characters. A critical comparative evaluation of the suitability of different popular equations of state including the Shanker, Poirier Tarantola, Bardeen and Srivastav-Pandey models was done to explain the high pressure behavior of $BiFeO_3$. In order to ensure the consistency and reliability, opposing parameters derived as pressure, bulk modulus, and derivatives of the former were systematically correlated with available experimental and theoretical data. We find that our proposed modified equation of state is better predicted and a more realistic description of the relationship between pressure and volume of $BiFeO_3$ at its compressed state. Its thermoelastic behavior can be

more explained by the theoretical framework owing to the fact that the modified formulation almost perfectly depicts the nonlinear changes in the elastic properties. Everything being as it is, the present model has much superior performance as compared to the present equations particularly in as far as replicating the experimental trend is concerned. This work aims to apply theoretical techniques, which are founded on a number of Equations of State (EOS) models, to investigate pressure-dependent thermoelastic behavior of bismuth ferrite ($BiFeO_3$). The analysis of the structural and elastic behavior of the material in different pressure conditions was performed using the Shanker, Poirier Tarantola, Bardeen, and Srivastav-Pandey EOS formulations. In addition, an isothermal EOS has the ability to determine the pressure derivative, bulk modulus, and the first derivative of the bulk modulus of the substance with little effort. [5].

Theory: To build a credible relationship between pressure, volume, and bulk modulus of high compression solids, the Shanker equation of state (EOS) [6-7] was created. This equation presents the elastic characteristics of materials at different pressure conditions, based on the principles of interatomic potential and incorporates the concept of finite strain theory.

$$P(V,T_0) = \frac{B_0}{2}\left[(B_0' - 3) - 2(B_0' - 2)\left(\frac{V}{V_0}\right)^{-1} + (B_0' - 1)\left(\frac{V}{V_0}\right)^{-2}\right] \quad (1)$$

where P is the pressure (in GPa), B_0 is the isothermal bulk modulus at zero pressure, B_0 is the derivative of isothermal bulk modulus at zero pressure, $\frac{V}{V_0}$ is the ratio of compressed volume(V) to initial volume(V_0).

A thermodynamically sound model known as the Poirier–Tarantola equation of state (EOS) [8-9] was created to explain the relationship between pressure and volume in solids at high pressures.

$$P = B_0\left(\frac{V}{V_0}\right)\left[\ln\frac{V_0}{V} + \left(\frac{B_0' - 2}{2}\right)\left(\ln\frac{V_0}{V}\right)^2\right] \quad (2)$$

One of the first theoretical models created to explain the connection between pressure and volume in solids under compression is the Bardeen equation of state (EOS) [10-11]. It was proposed by J. Bardeen and is based on the basic ideas of elastic material compressibility and interatomic potential energy. According to the Bardeen EOS, pressure can be calculated by differentiating a crystal's total energy with respect to volume and expressing this energy as a function of interatomic spacing. The Bardeen equation can be expressed in its general form as follows:

International Journal of Advance Interdisciplinary Research
Vol. 2, Issue 2, Part A, April-June) 2026, pp. 1-13, e-ISSN: 3107-913X
DOI:https://doi.org/10.66095/ijair.2026.v2.i2.a.1

$$P = 3fB_0(1+f^4)\left[1+\frac{3f}{2}(B_0'-3)\right] \quad (3)$$

where $\left[f = \left(\frac{V_0}{V}\right)^{1/3} - 1\right]$

The Srivastava–Pandey equation of state (EOS) [12] is a semi-empirical model proposed to improve the accuracy of pressure–volume predictions for solids under high compression.

$$P = B_0\left(\frac{V}{V_0}\right)^{-4/3}\left[\frac{\{\alpha^3(1+z+z^2+z^3)+\alpha^2(-3z^2-2z-1)+\alpha(6z+2)-6\}e^{\alpha z}-(\alpha^3-\alpha^2+2\alpha-6)}{\alpha^4}\right] \quad (4)$$

Where $z = 1-\frac{V}{V_0}$, $\alpha = \frac{3B_0'-8}{3}$

The expression for isothermal bulk modulus [13] can be given as

$$B_T = -V\frac{dP}{dV} = V\frac{d^2E}{dV^2} \quad (5)$$

Using equation (1) the equation of isothermal bulk modulus for Shanker EOS can be given as

$$B_T = B_0\left(\frac{V}{V_0}\right)\left[1+(B_0'+1)\left(1-\frac{V}{V_0}\right)\right] \quad (6)$$

Further using equation (2) for Poirier-Tarantola EOS, the expression for isothermal bulk modulus in case of Poirier-Tarantola EOS can be given as

$$B_T = B_0\left(\frac{V_0}{V}\right)\left[1+(B_0'-1)\ln\frac{V_0}{V}+\left(\frac{B'_0-2}{2}\right)\left(\ln\frac{V_0}{V}\right)^2\right] \quad (7)$$

Further using equation (3) for Bardeen EOS, the expression for isothermal bulk modulus in case of Bardeen EOS can be given as

$$B_T = B_0(1+f)^4\left[1+5f+\frac{3}{2}(B_0'-3)(2f+6f^2)\right] \quad (8)$$

Further using equation (4) for Srivastav-Pandey EOS, the expression for isothermal bulk modulus in case of Srivastav-Pandey EOS can be given as

$$B_T = B_0\left(\frac{V}{V_0}\right)^{-1/3}(1+z+z+z^2+z^3)exp(\alpha z)+\frac{4}{3}P \quad (9)$$

The expression for first derivative of isothermal bulk modulus [14-15] is given as

International Journal of Advance Interdisciplinary Research
Vol. 2, Issue 2, Part A, April-June) 2026, pp. 1-13, e-ISSN: 3107-913X
DOI:https://doi.org/10.66095/ijair.2026.v2.i2.a.1

$$B'_T = \frac{\partial B_T}{\partial P} \quad (10)$$

Using equation (1) and equation (6) in equation (10) the equation of first derivative of isothermal bulk modulus for Shanker EOS can be given as

$$B'_T = \left(\frac{V}{V_0}\right)(B'_0 + 1) - 1 \quad (11)$$

Further using equation (2) and equation (7) for Poirier-Tarantola EOS, the expression for first derivative of isothermal bulk modulus in case of Poirier-Tarantola EOS can be given as

$$B'_T = \left(\frac{B_0}{B_T}\right)\left(\frac{V_0}{V}\right)\left[B'_0 + (2B'_0 - 3)\ln\frac{V_0}{V} + \frac{B'_0 - 2}{2}\left(\ln\frac{V_0}{V}\right)^2\right] \quad (12)$$

Further using equation (3) and equation (8) for Bardeen EOS, the expression for first derivative of isothermal bulk modulus in case of Bardeen EOS can be given as

$$B'_T = \frac{B_0}{B_T}(1+f)^4\left[B'_0 + \frac{25}{3}f + 11(B'_0 - 3)f + 18(B'_0 - 3)f^2\right] \quad (13)$$

Further using equation (4) and equation (9) for Srivastav-Pandey EOS, the expression for first derivative of isothermal bulk modulus in case of Srivastav-Pandey EOS can be given as

$$B'_T = \left(1 - \frac{4P}{3B_T}\right)\left[\frac{1}{3} + \frac{V}{V_0}\left\{\alpha + \frac{1+2z+3z^2}{1+z+z^2+z^3}\right\}\right] + \frac{4}{3} \quad (14)$$

The Gruneisen parameter [16-18] is essential to comprehending the pressure dependence of the thermoelastic properties of $BiFeO_3$ in the current investigation. Compression-induced variations in γ shed light on how lattice dynamics and anharmonicity alter at high pressures. A comparative assessment of how well each EOS captures the anharmonic response of $BiFeO_3$ is made possible by the calculated values of the Gruneisen parameter using various equations of state (Shanker, Poirier–Tarantola, Bardeen, and Pandey–Srivastava). Vaschenko and Zubarev [19-20] introduced the free volume formula, which correlates the Gruneisen parameter with the isothermal bulk modulus and its pressure derivative, expressed as

$$\gamma_{ba-s} = \frac{\frac{B'_0}{2} - \frac{5}{6} + \frac{2}{9}\left(\frac{P}{B_0}\right)}{\left(1 - \frac{4P}{3B_0}\right)} \quad (15)$$

where P is the pressure, B_0 is the isothermal bulk modulus at zero pressure and B'_0 is the first order pressure derivative of the isothermal bulk modulus.

International Journal of Advance Interdisciplinary Research
Vol. 2, Issue 2, Part A, April-June) 2026, pp. 1-13, e-ISSN: 3107-913X
DOI:https://doi.org/10.66095/ijair.2026.v2.i2.a.1

For $BiFeO_3$, which has a unique structure known as the rhombohedral perovskite structure, the lattice parameter [21] was examined and was found to regularly decrease as pressure increased, indicating that it is functioning normally. This decrease was attributed to the Fe–O and Bi–O bond lengths becoming shorter, which raised the structural rigidity and bulk modulus.

$$a = a_0 \left(1 + B_0' \frac{P}{B_0}\right)^{\frac{-1}{B_0'}} \quad (16)$$

where a is the lattice parameter at atmospheric pressure and a is the lattice parameter under high pressure.

Result and Discussion: Four distinct equations of state (EOS)—Shanker, Poirier–Tarantola, Bardeen, and Srivastava–Pandey EOS—have been used to study the variation of pressure, isothermal bulk modulus, its pressure derivative, Gruneisen parameter, and lattice parameter with the compression ratio (V/V_0) for bismuth ferrite ($BiFeO_3$). These EOS shed light on the material's structural stability, anharmonic behavior, and thermodynamic characteristics while describing its elastic response under isotropic compression. Normal compressional behavior is indicated by the P–V/V_0 relationship, which displays a typical nonlinear increase in pressure as volume decreases based on the computed data. In the low-pressure region, the various EOS models exhibit strong agreement; however, at high compression, they slightly diverge, indicating model-dependent stiffness predictions. Lattice stiffening [22] and decreased compressibility at high pressures are confirmed by the bulk modulus (B), which steadily rises as volume decreases. However, the pressure derivative of the bulk modulus (B'_T) gradually drops, suggesting that internal rearrangements in the Bi–O–Fe network cause a slight reduction in resistance to additional compression. Increased anharmonicity and phonon coupling effects are indicated by the Gruneisen parameter (γ), which exhibits a steady pattern at low pressure and a sharp increase around $V/V_0 \approx 0.71$. Furthermore, a regular contraction of the unit cell under compression is confirmed by the lattice parameter (a), which decreases linearly with decreasing volume ratio. The best EOS available is the Shanker EOS. In every parameter, it exhibits the smoothest and most physically consistent behavior. The thermoelastic characteristics of $BiFeO_3$ over a broad compression range are well described by this EOS. The isothermal bulk modulus at zero pressure (B_0) and its first pressure derivative (B'_0) were determined to be 97.3GPa and 4.6GPa, respectively from references [23-25], for the purposes of this analysis. To guarantee consistency and comparability of results across the various models, these constants were used as the reference input parameters in all EOS formulations.

Causes of deviation under high compression:

1.Anharmonicity suppression: The interatomic potential well becomes more symmetrical and steeper at high compression. The anharmonic contribution decreases as phonon frequencies harden (increase quickly). This causes it to drop from its almost ambient value.

2.Electronic structure changes: Under high pressure, electron density redistributes, which can occasionally result in changed ion-ion interaction screening and s–p–d electron transfer. These cause anomalies by altering the pressure dependence of vibrational frequencies.

3.Structural phase transitions: Materials frequently undergo denser crystalline phases as a result of high compression. Changes in lattice symmetry result in sudden changes in the phonon spectrum. This results in significant deviations or abrupt jumps.

4. Soft-mode behavior: In some systems, pressure causes some phonon branches to soften before a new phase is stabilized. These vibrons diverge locally due to their unusual pressure dependence.

5. Equation of state nonlinearity: The basic Mie–Gruneisen EOS assumes smooth variations. The assumption fails at high compression because higher-order terms in the EOS become significant. The experimental and ideal models deviate systematically as a result.

6. Electron-phonon coupling: This can become stronger at very high compression, particularly in the vicinity of metallization. This changes the effective by modifying the contributions of vibrational pressure.

7. Ionic and molecular dissociation: High pressure in solids can cause molecules to reorient or break bonds. The average phonon frequency–volume relationship is significantly impacted as a result of the introduction of new vibrational modes and the elimination of old ones.

International Journal of Advance Interdisciplinary Research
Vol. 2, Issue 2, Part A, April-June) 2026, pp. 1-13, e-ISSN: 3107-913X
DOI:https://doi.org/10.66095/ijair.2026.v2.i2.a.1

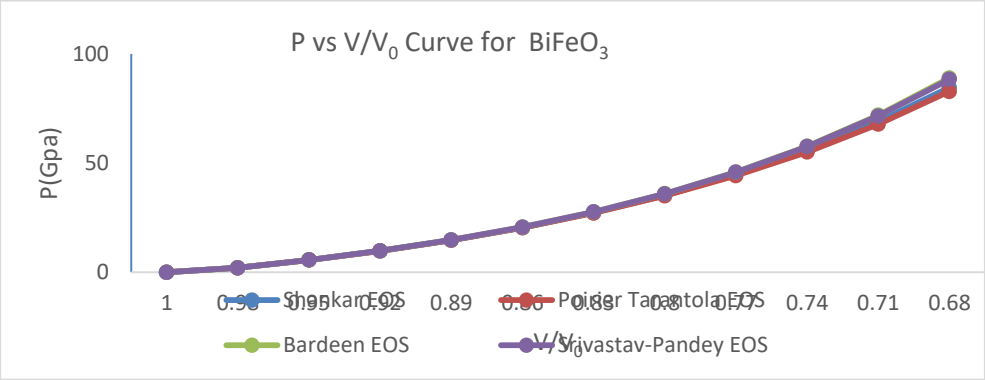

The graph above illustrates the relationship between pressure, (P) and volume compression ratio, (V/V 0) of three different equations of state (EOS) of the material $BiFeO_3$ namely Shanker, Poirier-Tarantola, Bardeen and Srivastava-Pandey EOS. The non-linear nature of the pressure-volume compression ratio (V/V_0) ratio, versus the volume compression ratio, of all equations of state is an indication of the expected compressive behavior of $BiFeO_3$. The Srivastava-Pandey EOS predicts higher pressure at more compression than either of the other two curves, a sign of a higher stiffness, but all three curves intersect near the equilibrium point ($V/V_0 = 1$). Along the way the Shanker and Bardeen EOS remain nearer to each other, meaning better the agreement in the medium-pressure regime and confirming the existence of the elastic stability of $BiFeO_3$ under compression. According to the trend, $BiFeO_3$ possesses a large degree of compressional structural stability.

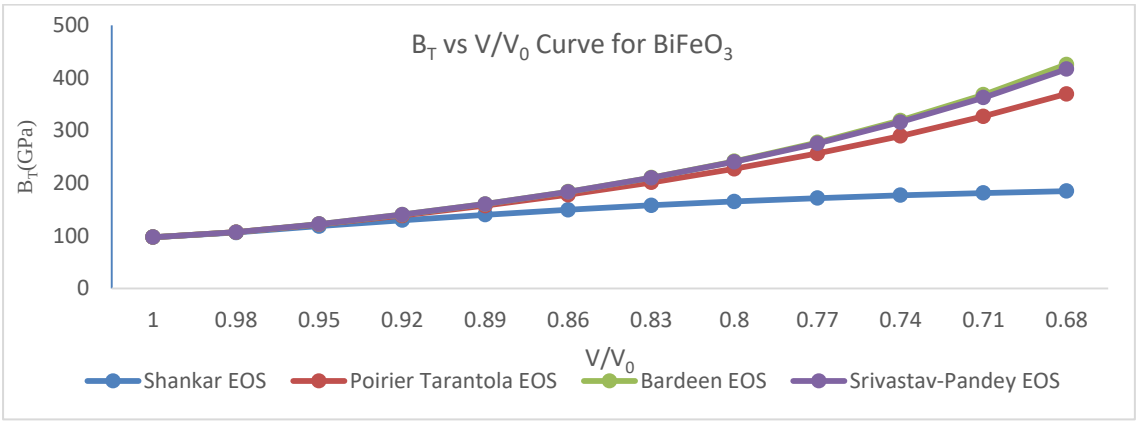

Figure.2 Isothermal bulk modulus (B_T) vs Volume compression ratio(V/V_0) Curve for $BiFeO_3$

Figure 2 shows the correlation between the bulk modulus (B_T) and the volume compression ratio (V/V_0). The isothermal bulk modulus is a graph between the volume compression ratio (V/V_0) that is a measure of the resistance of a material to uniform compression. When $BiFeO_3$ is in compressed form, it is clear that the bulk modulus increases. Srivastava-Pandey EOS and Shanker EOS give highest and lowest predictions respectively. The intermediate predictions of the experimentally closer Bardeen

International Journal of Advance Interdisciplinary Research
Vol. 2, Issue 2, Part A, April-June) 2026, pp. 1-13, e-ISSN: 3107-913X
DOI:https://doi.org/10.66095/ijair.2026.v2.i2.a.1

EOS and Poirier Tarantola EOS are likely to be closer to the experimental reality.

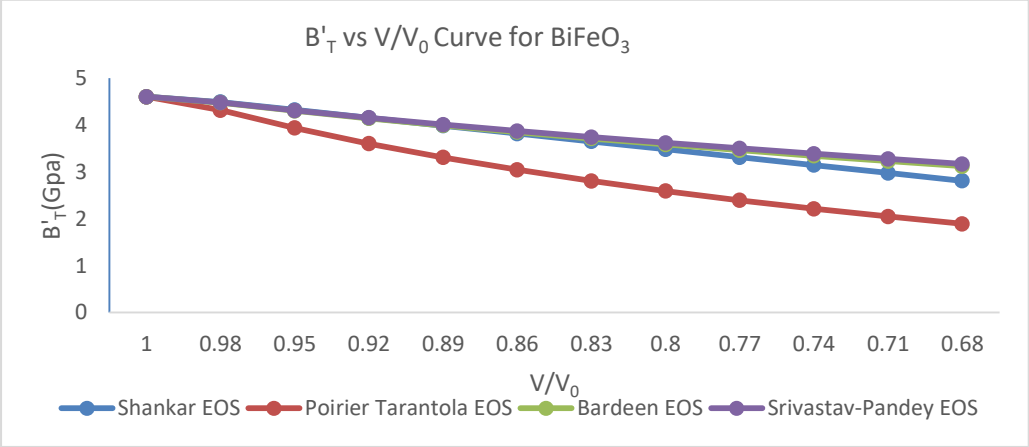

Figure.3 First derivative of isothermal bulk modulus (B'_T) vs Volume compression ratio(V/V_0) Curve for $BiFeO_3$

Figure 3 shows the influence of the volume compression ratio (V/V_0) on the first derivative of the bulk modulus (K_T). The Shanker, Poirier-Tarantola, Bardeen and Srivastav-Pandey EOS were used to determine the bulk modulus. With decrease in the volume compression ratio, the graph indicates that Shankar foresees moderate decrease in the bulk modulus. Unlike the others, Poirier has a much lower value of high compression bulk modulus. Srivastav and Pandey EOS yield the largest bulk modulus in the range, and Bardeen yields a comparatively stronger (less compressible) material than the rest. Overall, there are certain differences in the predicted values; however, the findings of the three different methods reveal that the bulk modulus is less when the volume compression ratio is high.

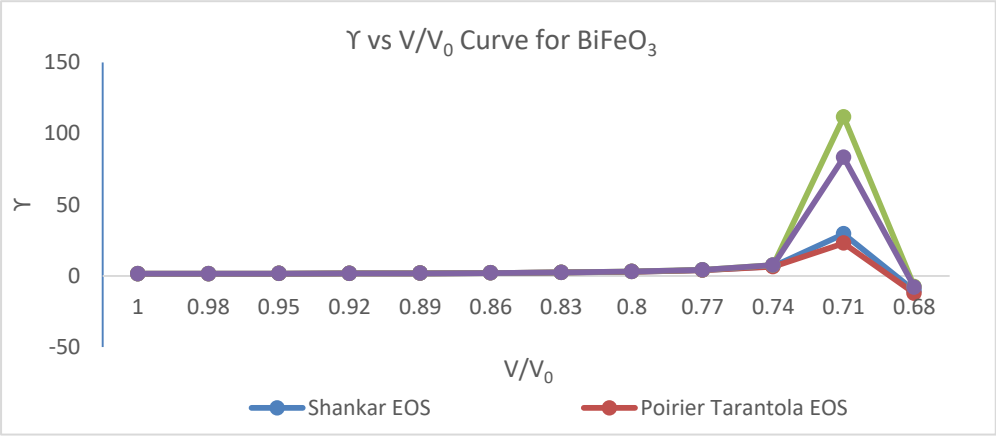

Figure.4 Gruneisen parameter($\gamma_{ba\text{-}s}$) vs Volume compression ratio(V/V_0) Curve for $BiFeO_3$

The correlation between the volume compression ratio(V/V_0) and the Gruneisen parameter($\gamma_{ba\text{-}s}$) is represented in the graph of Figure 4. It is possible to observe that curves are closer to zero at a larger volume ratio (approximately 1.0, which is the state of equilibrium) implying the lowest change. The equations of state predictions are however widely differentiated at high compression which is manifested by the sharp peak near 0.71-0.74 of all the models as the volume ratio decreases (i.e. compression is increasing).

International Journal of Advance Interdisciplinary Research
Vol. 2, Issue 2, Part A, April-June) 2026, pp. 1-13, e-ISSN: 3107-913X
DOI:https://doi.org/10.66095/ijair.2026.v2.i2.a.1

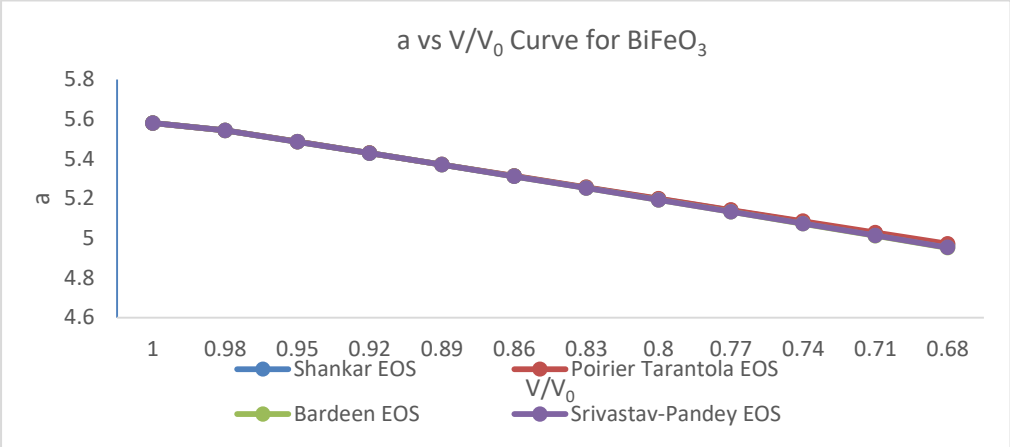

Figure.5 Lattice parameter(a) vs Volume compression ratio(V/V_0) Curve for $BiFeO_3$

The volume compression ratio (V/V_0) versus Lattice parameter (a) is depicted in (Fig. 5) graph. The lattice parameter (a) is a measure of uniform lattice contraction and it is linearly proportional to compression. The fact that all the EOS curves overlap closely is testimony to the reliability of the models and their consistency. The linear change in variation of a confirms that the compression is completely elastic without structural deformation in the studied range and indicates the argued structural stability of $BiFeO_3$. It is also proportional to the increase in bulk modulus that was observed. Conclusion: All four EOS formulations satisfactorily replicate the overall compression trend of $BiFeO_3$. However, at least to predict the thermoelastic behavior of $BiFeO_3$, the Shankar EOS offers smoother and more physically consistent behavior throughout all parameters, and in particular at moderate pressures. The isothermal bulk modulus (B_T) displays the lattice stiffening, which increases continuously with compression, although the first derivative of its pressure decreases slightly, which reflects some slight structural changes at high pressure. The absence of anharmonicity at high compression is manifested in the non-linear behaviour of the Gruneisen parameter (γ) with an initial magnitude of increase that is followed by a subsequent decrease. The homogeneous contraction and integrity of $BiFeO_3$ is further aided by the continuous reduction in the lattice parameter with pressure. The anticipated results show good correlation with the theoretical information available proving the suitability of the adopted methodology to analyze the thermodynamic and elastic behavior of $BiFeO_3$.

International Journal of Advance Interdisciplinary Research
Vol. 2, Issue 2, Part A, April-June) 2026, pp. 1-13, e-ISSN: 3107-913X
DOI:https://doi.org/10.66095/ijair.2026.v2.i2.a.1

V/V0	P(GPa) B'T(GPa) (s)	P(GPa) (p)	P(GPa) B'T(GPa) (b)	P(GPa) (s-p)	BT(GPa) B'T(GPa) (s)	(p)	BT(GPa) B'T(GPa) (b)	(s-p)	BT(GPa) (s)	(p)	BT(GPa) (b)	(s-p)
1.00	0.00	0.00	0.00	0.00	97.30	97.30	97.30	97.30	4.60	4.60	4.60	4.60
0.98	2.06	2.06	2.06	2.06	106.03	106.56	106.64	106.64	4.49	4.32	4.48	4.48
0.95	5.61	5.60	5.61	5.61	118.32	121.68	122.24	122.25	4.32	3.94	4.30	4.31
0.92	9.79	9.77	9.82	9.82	129.62	138.46	140.02	140.01	4.15	3.60	4.14	4.15
0.89	14.70	14.67	14.79	14.79	139.94	157.12	160.34	160.29	3.98	3.31	3.99	4.01
0.86	20.48	20.41	20.68	20.68	149.28	177.92	183.64	183.46	3.82	3.04	3.85	3.87
0.83	27.28	27.13	27.67	27.65	157.64	201.16	210.45	210.00	3.65	2.81	3.71	3.74
0.80	35.27	35.01	35.97	35.94	165.02	227.20	241.41	240.47	3.48	2.59	3.58	3.62
0.77	44.69	44.25	45.88	45.78	171.42	256.48	277.31	275.51	3.31	2.39	3.46	3.50
0.74	55.81	55.09	57.71	57.52	176.84	289.51	319.11	315.91	3.14	2.21	3.34	3.39
0.71	68.96	67.83	71.91	71.55	181.27	326.91	368.03	362.60	2.98	2.05	3.23	3.28
0.68	84.57	82.85	89.01	88.35	184.73	369.42	425.57	416.71	2.81	1.89	3.12	3.17

Table1: Calculated values pressure(P), isothermal bulk modulus (B_T), its first pressure derivative (B_T), at different compressions(V/V_0) for $BiFeO_3$ using (s) Shanker EOS, (p) Poirier Tarantola EOS, (b) Bardeen EOS and (s-p) Srivastav-Pandey EOS

Table 2: Calculated values Barton-Stacey Gruneisen parameter($\gamma_{ba\text{-}s}$) and Lattice parameter at different compressions(V/V_0) for $BiFeO_3$ using (s) Shanker EOS, (p) Poirier Tarantola EOS, (b) Bardeen EOS and (s-p) Srivastav-Pandey EOS

V/V_0	$\gamma_{(ba\text{-}s)}$ (s)	$\gamma_{(ba\text{-}s)}$ (p)	$\gamma_{(ba\text{-}s)}$ (b)	$\gamma_{(ba\text{-}s)}$ (p-s)	$a(A^0)$ (s)	$a(A^0)$ (p)	$a(A^0)$ (b)	$a(A^0)$ (p-s)
1.00	1.47	1.47	1.47	1.47	5.58	5.58	5.58	5.58
0.98	1.51	1.51	1.51	1.51	5.54	5.54	5.54	5.54
0.95	1.60	1.60	1.60	1.60	5.49	5.49	5.49	5.49
0.92	1.72	1.72	1.72	1.72	5.43	5.43	5.43	5.43
0.89	1.88	1.88	1.88	1.88	5.37	5.37	5.37	5.37
0.86	2.10	2.10	2.11	2.11	5.31	5.31	5.31	5.31
0.83	2.44	2.43	2.46	2.46	5.25	5.26	5.25	5.25
0.80	2.99	2.97	3.05	3.05	5.20	5.20	5.19	5.19
0.77	4.05	3.98	4.23	4.22	5.14	5.14	5.13	5.13
0.74	6.78	6.50	7.64	7.55	5.08	5.08	5.07	5.07
0.71	29.53	23.01	111.62	83.20	5.02	5.03	5.01	5.01
0.68	-10.44	-12.24	-7.60	-7.92	4.97	4.97	4.95	4.95

References:

1. Shirane G., Sawaguchi E., and Takagi Y., Phys. Rev. 84, 476-483 (1951)

2. Shirane G., and Pepinsky R., Phys. Rev. 91, 812-815 (1953)

3. Zvezdin A.K., Pyatakov A.P., Phys. Usp. 55(6), 557-581 (2012)

4. Shang S. L., G Sheng., Y Wang., Chen L. Q., and Liu Z. K., Phys. Rev. 80, 052102-1-052102-4 (2009)

5. Singh S.P., Pramana-J. Phys. 96, 74 (2022)

6. Tripathi S., Pandey A.K., Srivastava S., Singh P., Dixit C.K., Der Pharma Chemica 15, 32-41 (2023)

7. Shanker J., Kushwaha S.S., Sharma M.P., Physica B 271, 158 (1999)

8. Poirier. J.P., Introduction to Physics of Earth's Interior (Cambridge Univ. Press, Cambridge, 1991)

9. Tripathi, S., Bharti, A.S., Uttam, K.N. et al. J Math Chem 63, 222–236 (2025).

10. Tripathi, S., Bharti, A.S., Pandey, A.K., Dixit, C.K., J Math Chem 62, 2265–2279 (2024).

11. S.P. Singh, Indian Acad. Sci., 126, (2017)

12. Srivastav, A.P., Pandey, B.K., 8, 152-166 (2024)

13. Srivastava A.P., Pandey B.K., Gupta A. K., Pandey A.K., J. Math. Chem. https://doi.org/10.1007/s10910-024-01647-z

14. Stacey F.D., Davis P.M., Phys. Earth Planet. Inter. 142, 137 (2004)

15. Kumar M., Subramanian S. S., Gaurav S., Int. J. 3, 536-541 (2014)

16. Tripathi S., Bharti A.S., Pandey A.K., and Dixit C.K. Analysis of high pressure equation of state for gallium compounds. page no.211-234, Emerging Technology and materials in Thermal Engineering, Book Title- High-Pressure Thermoelastic and Thermophysical Properties of Smart Materials, Edited by- Pandey A K, Dixit C. K., Srivastava S.

17. Spectroscopic estimation of thermodynamic properties of copper monohalides (CuF, CuCl, CuBr, and CuI), Tripathi S., Pandey A. K., Kailash N.U., Dixit C. K., SciEngg Advances, 2024, Vol. 1, No. 3, 116-123, ISSN: 3064-6758, Ariston Publications 2024

18. Tripathi, S., Srivastava, S., Singh, P., Pandey, A., K. and Dixit, C., K., Analysis of High Pressure EOS on the Structural Properties of Gallium Compounds. The Green Revolution: Building Sustainable Solutions: 3rd International Conference on Resent Trends in Environment and Sustainable Development, Ed: Kumud Kant Awasthi, Subodh Srivastava, Sushila Rathore, Springer Cham, ISBN 978-3-031-93444-5, 2025

19. Pandey B.K., Pandey A.K., Singh C.K., AIP Conf. Proc. 1, 120004 (2008)

20. Pandey A.K., Singh P., Srivastava S., Tripathi S., Dixit C.K., J. Nanomaters. Mol. Nanotechno. 12, 1 (2023)

21. Lattice parameter Sirwan K., Jalal A.M. Al-S. Raf. J. Sci., 25, 80- 89, (2014)

22. Jian G., Xue F., Guo Y., Yan C., Materials doi:10.3390/ma11122441, (2018)

23. Gaurav S., Shankar Subramanian S., Singh Satyendra P., and, Sharma B.S., Condensed Matter and Materials Science July 2012.

24. Pandey A.K., Pandey B.K., Singh C.K., Srivastava A.P., Elixir Crystal Research Tech. 44(C), 7420 (2012)

25. Zhu J.L., Feng S.M., Wang L.J., Int. J. 30, 265-272 (2010).